Concerning the Design of Capacitively Driven Induction Coil Guns

JIANLIANG HE, STUDENT MEMBER, IEEE, ENRICO LEVI, SENIOR MEMBER, IEEE, ZIVAN ZABAR, SENIOR MEMBER, IEEE, AND LEO BIRENBAUM, SENIOR MEMBER, IEEE

Abstract—**This paper is concerned with the design of capacitively driven, multisection, electromagnetic coil launchers, or coil guns, taking their transient behavior into account. A computer simulation based on the viewpoint of lumped parameter circuits is developed to predict the performance of the launcher system. It is shown that a traveling electromagnetic wave can be generated on the barrel by the resonance of drive coils and their capacitors. More than half of the energy initially stored in the capacitor bank can be converted into kinetic energy of the projectile in one shot, and an additional quarter can be utilized in subsequent shots, if the launcher dimensions, resonant frequency, and firing sequence are properly selected. The projectile starts smoothly from zero initial velocity and with zero initial sleeve current. Section-to-section transitions which have significant effects on the launcher performance are also discussed. Experimental results were obtained with a small model and are in good agreement with theoretical predictions.**

I. Introduction

An advantage that electromagnetic launchers have over chemical ones is that they can accelerate projectiles to much higher (hyper) velocities. The present interest in electromagnetic launchers has resulted in a great competition between the two major types: Rail guns and coil guns. Although rail guns are currently at a more advanced stage of development, coil guns have their own desirable characteristics which have been discussed in the literature [1]–[5]. The operating principles of various kinds of coil launchers have been summarized by Mongeau *et al.* [2]. The performance of such launchers is still being investigated. In a previous paper [4], design principles based on the assumption that a steady state prevails in each section of the gun were outlined. Here, instead, account is taken of the fact that the steady state is actually never reached during the transit of the projectile through the gun.

The first part of this paper describes the physical arrangement and the computer simulation model. The second part discusses the design. Numerical results and performance estimates for a launcher now under construction are given in the third part, which contains also a comparison between theoretical predictions and experimental data obtained with a small laboratory model.

Manuscript received October 14, 1988; revised February 8, 1989. This work was supported by the SDIO/IST and managed by the AFOSR under Contract no. F49620-86-C-0126 and by the USASDC under Contract no. DASG60-88-C-0047.

The authors are with the Polytechnic University, 333 Jay Street, Brooklyn, NY 11201.

IEEE Log Number 8927934.

II. Theory and Simulation Model

A. Capacitively Driven Coil-Launcher System

Fig. 1 is a sketch of a capactively driven, multisection coil launcher which consists of two main parts: The barrel and the projectile. It may be driven either by a set of capacitors, as indicated in the diagram, or, alternatively, by a set of ac polyphase sources. The barrel is a linear array of drive coils. The projectile is a conducting sleeve surrounding the payload. The drive coils on the barrel are energized with a certain time sequence so as to generate a traveling electromagnetic wave that interacts with a system of currents in the sleeve.

Two modes of operation are possible for the launcher: The "synchronous" mode and the "asynchronous" mode. In the first case, the velocity of the projectile is exactly equal to that of the traveling wave. For this mode a set of currents must be impressed on the sleeve; each coil must be energized separately; the timing of the closure of each switch must be governed by the position of the projectile; and the size of each capacitor must be chosen in such a way that the frequency matches the dM/dx curves of the drive coils. Because of the complexity of the control system and the power conditioner associated with this mode, we discuss instead in detail here the asynchronous mode in which the projectile velocity is smaller than that of the traveling wave so that the relative motion between the two causes induced currents in the projectile. In this case the coils may be connected in series or in parallel to form a limited number of phase windings, as is done in conventional machines. However, since the losses in the sleeve are proportional to its "slip" behind the traveling wave, and since, in a launcher, the projectile velocity ranges over at least one order of magnitude, it becomes necessary to increase the velocity of the traveling wave stepwise by dividing the barrel into sections. In order to obtain a wave whose phase velocity increases from section to section along the length of the barrel, either the frequency f or the pole pitch (half wavelength) must increase. Because of the relatively short length of the projectile it is not practical to increase the pitch adequately. Therefore the resonant frequency must increase along the length of the barrel and different capacitor sizes must be used in different sections.

B. System Equations

The coil launcher of Fig. 1 is modeled by the equivalent circuit shown in Fig. 2. Because the axial distribution of

0093-3813/89/0600-0429$01.00 © 1989 IEEE

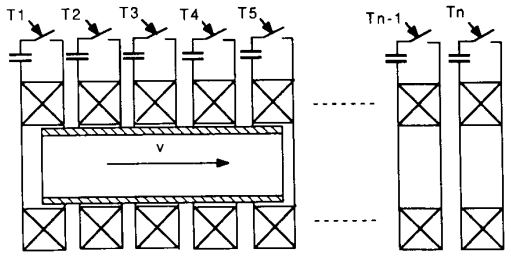

Fig. 1. Sketch of multisection capacitively driven coil launcher.

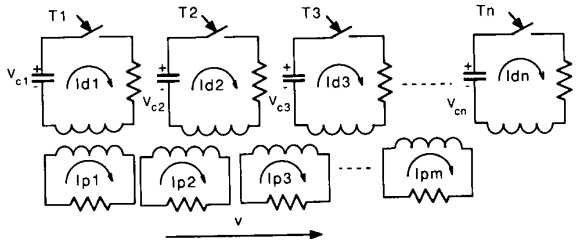

Fig. 2. Lumped parameter circuit model of the capacitively driven coil launcher.

the induced current in the sleeve is not uniform, to simulate the physical system we divide the sleeve into several zones that are electrically insulated from each other and represent them as separate projectile coils. The number of coils into which we divide the sleeve depends on the requirement of accuracy. The number of drive coils depends on performance specifications such as the muzzle velocity, weight of the projectile, the caliber, and the length of the barrel. We denote by n the number of drive coils, and by m the number of projectile coils.

Employing Kirchhoff's voltage law, we write the network equations in matrix form:

$$[V] = [R][I] + \frac{d}{dt}\{[L][I] + [M][I]\} \quad (1)$$

where $[V]$ and $[I]$ are column ($m + n$ element) matrices composed of the individual projectile and drive-coil voltages and currents, respectively. $[R]$ and $[L]$ are diagonal ($m + n$ element) matrices composed of the individual projectile and drive-coil resistances and self-inductances, respectively, and $[M]$ is a square $(m + n) \times (m + n)$ matrix, each element of which represents a mutual inductance between any two individual coils. The formulas used to evaluate each element of $[L]$ and $[M]$ are given in [6] and [7]. It should be noted that the mutual inductances $[M]$ between drive coils and projectile coils are functions of the distance x which denotes the position of the projectile and is a function of time. This complicates matters considerably.

The relations between the capacitor voltages and drive-coil currents are

$$[C]\frac{d}{dt}[V_c] = -[I_d] \quad (2)$$

where $[C]$ is a diagonal (n element) matrix containing the capacitances and $[V_c]$ and $[I_d]$ are the capacitor voltage and the drive-coil current column matrices, respectively. $[V_c]$ and $[I_d]$ are submatrices of $[V]$ and $[I]$.

The Lorentz force acting on the projectile is given by

$$F = \tfrac{1}{2}[I]^T[G][I] \quad (3)$$

where $[G] = d[M]/dx$ and the superscript T stands for the transpose of the matrix. Finally, we consider the equation of motion and combine it with (1)–(3). The complete set of equations which describe the capacitively driven coil-launcher system is then given in matrix form:

$$\{[L] + [M]\}\frac{d}{dt}[I] = [V] - [R][I] - v_p[G][I] \quad (m + n \text{ eqns.}) \quad (4)$$

$$[C]\frac{d}{dt}[V_c] = -[I_d] \quad (n \text{ eqns.}) \quad (5)$$

$$M_p\frac{dv_p}{dt} = \sum_{p=1}^{m}\sum_{d=1}^{n} I_p I_d \frac{dM_{pd}}{dx} \quad (1 \text{ eqn.}) \quad (6)$$

$$\frac{dx}{dt} = v_p \quad (1 \text{ eqn.}) \quad (7)$$

where M_p is the mass of projectile and v_p is the velocity of the projectile. Equations (4)–(7) represent a set of simultaneous nonlinear differential equations with time-variable coefficients. The number of first-order differential equations involved in the system is

$$N = 2n + m + 2 \quad (8)$$

in $2n + m + 2$ variables (m projectile currents, n drive currents, n driver capacitor voltages, v_p, and x).

C. Analysis of the System Energies

To assess the performance of the launcher system one needs first to consider the energy balance relations. This will eventually lead to the optimum design of the launcher. Basically, the energy balance involves several items: The electric energy stored in the capacitor bank, the magnetic energy stored in the coils, the kinetic energy gained by the projectile, and the ohmic loss due to the resistances. The main goal in the design of a capacitively driven coil launcher is to achieve the transfer of as much as possible of the electric energy stored in the capacitors into kinetic energy of the projectile to attain high system efficiency. The energy relations are derived as follows below.

Multiplying (1) by $[I]^T$ and rewriting it in an alternative form, we obtain:

$$[I]^T[V] = [I]^T[R][I] + [I]^T\{[L] + [M]\}\frac{d}{dt}[I] + [I]^T v_p[G][I]. \quad (9)$$

Since

$$\frac{d}{dt}\left\{\frac{1}{2}[I]^T([L]+[M])[I]\right\} = [I]^T([L]+[M])\frac{d}{dt}[I] + \frac{1}{2}\left\{[I]^T v_p[G][I]\right\} \tag{10}$$

(9) can be rewritten as

$$[I]^T[V] = [I]^T[R][I] + \frac{d}{dt}\left\{\frac{1}{2}[I]^T([L]+[M])[I]\right\} + \frac{1}{2}v_p[I]^T[G][I]. \tag{11}$$

We note in (11) that the term on the left represents the electric power in the capacitor. The first term on the right-hand side represents the ohmic loss of the system, the second term represents the time rate of change of the magnetic energy stored in the coils, and the last term represents the converted power. Then the energy balance at time t can be derived from the power balance equation by integrating (11) in time to obtain:

$$W_{\text{cap}} = W_{\text{ohm}} + W_{\text{mag}} + W_{\text{conv}} \tag{12}$$

where

$$W_{\text{cap}} = \int_0^t [I]^T[V]\,dt' + \sum_{i=1}^{n}\frac{1}{2}C_i V_i^2(0) \tag{13}$$

$$W_{\text{ohm}} = \int_0^t [I]^T[R][I]\,dt' \tag{14}$$

$$W_{\text{mag}} = \frac{1}{2}\int_0^t \frac{d}{dt'}\left\{[I]^T([L]+[M])[I]\,dt'\right\} = \frac{1}{2}[I]^T([L]+[M])[I] \tag{15}$$

$$W_{\text{conv}} = \frac{1}{2}\int_0^{T_p}[I]^T v_p[G][I]\,dt' = \frac{1}{2}\int_0^{l}[I]^T[G][I]\,dx \tag{16}$$

where l is the length of the barrel and T_p stands for the total time the projectile needs to travel along the barrel. The prime notation is used to distinguish between the variable of integration t' and the upper limit t.

We observe from the integrands in (16) that the force on the projectile is

$$F = \frac{1}{2}[I]^T[G][I] = \sum_{p=1}^{m}\sum_{d=1}^{n} I_d I_p \frac{dM_{dp}}{dx} \tag{17}$$

which is the result we have used in the previous section. Since the system is time varying, we define an average acceleration

$$a_{\text{av}} = \frac{1}{T_p}\int_0^{T_p}\frac{\sum_{p=1}^{m}\sum_{d=1}^{n} I_d I_p \frac{dM_{dp}}{dx}}{M_p}\,dt. \tag{18}$$

This average acceleration, as calculated by the simulation code, is an important quantity for the design of the launcher because it affects the dimensions of the launcher. Another key quantity is the Energy Transfer Ratio (ETR), which is defined as the ratio of the gain in kinetic energy to the total energy initially stored in the capacitors, because it affects the weight of the capacitor bank:

$$\text{ETR} = \frac{W_{\text{kf}} - W_{\text{ki}}}{W_{\text{cap}}(0)} = \frac{W_{\text{conv}}}{W_{\text{cap}}(0)} = \frac{\frac{1}{2}M_p(v_f^2 - v_i^2)}{\sum_{d=1}^{n}\frac{1}{2}C_d V_{cd}^2(0)} \tag{19}$$

where W_{kf} and W_{ki} refer to the final and initial kinetic energies of the projectile respectively, $W_{\text{cap}}(0)$ stands for initial capacity energy, v_f and v_i are the final and initial velocities of the projectile, and $V_{cd}(0)$ is the initial capacitor voltage. Finally, an Energy Loss Ratio (ELR) is defined as

$$\text{ELR} = \frac{W_{\text{ohm}}}{W_{\text{cap}}(0)}. \tag{20}$$

Separating the ohmic losses of the projectile coils and the drive coils and using (14), one obtains

$$W_{\text{ohm}} = W_{\text{ohm}}^p + W_{\text{ohm}}^d \tag{21}$$

$$W_{\text{ohm}}^p = \int_0^{T_p}\sum_{p=1}^{m} R_p I_p^2\,dt \tag{22}$$

$$W_{\text{ohm}}^d = \int_0^{T_d}\sum_{d=1}^{n} R_d I_d^2\,dt \tag{23}$$

where T_d is the energization (oscillation) time of a single section. This time may differ from one section to another.

Using (21)–(23), one can write (20) as

$$\text{ELR} = \frac{\int_0^{T_p}\sum_{p=1}^{m} R_p I_p^2\,dt + \int_0^{T_d}\sum_{d=1}^{n} R_d I_d^2\,dt}{\frac{1}{2}\sum_{d=1}^{n} C_d V_{cd}^2(0)}. \tag{24}$$

The temperature rise in the launcher can be derived from (22) and (23). If $V_{\text{vol},p}$ is the volume of a projectile coil, $V_{\text{vol},d}$ the volume of a drive coil, $c(JK^{-1}m^{-3})$ the specific heat of the material, and θ_p, θ_d the temperature rise of each projectile coil and drive coil, respectively, and if one assumes that the launch time is so short that the process is nearly adiabatic, then one obtains

$$\theta_p = \frac{\int_0^{T_p} R_p I_p^2\,dt}{cV_{\text{vol},p}} \qquad p = 1, m \tag{25}$$

$$\theta_d = \frac{\int_0^{T_d} R_d I_d^2\,dt}{cV_{\text{vol},d}} \qquad d = 1, n. \tag{26}$$

If one assumes that the volumes of all the projectile coils are the same, then the average temperature rise in

the projectile sleeve is

$$\langle \theta_p \rangle = \frac{\sum_{p=1}^{m} \theta_p}{m} = \frac{\sum_{p=1}^{m} \int_0^{T_p} R_p I_p^2 \, dt}{mcV_{\text{vol},p}}. \tag{27}$$

Likewise, if one assumes that all the drive coils have the same volume and that the time T_d (that each drive coil is energized) is the same, then one can define the average temperature rise of the drive coils as

$$\langle \theta_d \rangle = \frac{\sum_{d=1}^{n} \theta_d}{n} = \frac{\sum_{d=1}^{n} \int_0^{T_d} R_d I_d^2 \, dt}{ncV_{\text{vol},d}}. \tag{28}$$

III. Design of a Capacitively Driven Coil Launcher

Design Considerations

The major considerations in designing a capacitively driven coil launcher are to determine the launcher dimensions, capacitor sizes, and the firing sequence needed from the power condition so that a traveling magnetic wave can be generated and a maximum energy transfer ratio can be obtained, while the mechanical and thermal stresses are kept within the allowable limits for a given material.

Unlike the case of most classical electric machines, in the capacitively driven multisection coil launcher the traveling wave is generated by the resonance of the drive coils and their capacitors. In addition, there are some peculiar problems. The traveling wave is a wave packet with finite length and attenuation in time. This creates many time and space harmonics. The attenuation strongly depends on the coupling between the barrel and sleeve and on their time constant. Good coupling gives good energy transfer but high attenuation. The phase currents are asymmetrical due to the asymmetrical mutual inductances between the phases. This causes energy transfer between neighboring drive coils to occur and a different Capacitor Discharge Ratio (CDR) (the ratio of final-to-initial capacitor energy storage) to exist in each phase. Besides, the resonant frequencies and the phase shifts in each phase winding vary with the time and the position of the projectile sleeve; in fact, the natural behavior of the coupled oscillators tends to eliminate the phase shifts between the phase currents and thus kills the traveling wave on the barrel. To design high-performance capacitively driven coil launchers one should take all of the above problems into consideration. First, for given dimensions one can calculate the energy transfer ratio, the average acceleration, and the velocity gain in each section of the barrel. These, in turn, lead to the determination of the quantities which follow below.

1) Determination of Barrel Length: To estimate the total length of a multisection barrel one can assume that the average acceleration is constant for every section. This assumption is based on the following consideration: For the best utilization of the barrel one must maximize the force acting on the projectile and, therefore, its acceleration, consistent with the maximum allowable mechanical and thermal stress. Then the kinetic energy gain W_{kj} in each drive-coil section is proportional to the length of the section, and may be expressed as

$$W_{\text{kj}} = M_p \alpha_{\text{av}} l_j \tag{29}$$

where the subscript j stands for the jth section, l_j stands for the length of the jth section, and W_{kj} is defined as

$$W_{\text{kj}} = \tfrac{1}{2} M_p (v_j^2 - v_{j-1}^2) \tag{30}$$

so that

$$l_j = \frac{\tfrac{1}{2}(v_j^2 - v_{j-1}^2)}{\alpha_{\text{av}}} \tag{31}$$

$$= \frac{2v_{j-1}v + v^2}{2\alpha_{\text{av}}} \tag{32}$$

where $v = v_j - v_{j-1}$ is the velocity increment per section, a quantity which is a system specification. v_{j-1}, v_j stands for the entering and exit velocities of the jth section, respectively. The total length of the barrel is the summation of the section lengths:

$$l = \sum_{j=1}^{N_s} l_j \tag{33}$$

where N_s is the number of sections.

It should be noted that the average acceleration α_{av} used in the above equations is selected on the basis of the maximum allowable mechanical stress and represents an initial input to the computer before the simulation is carried out. The energies stored initially in the capacitors of each section are then adjusted during the simulation so as to yield corrected average accelerations from (18) which match those of (29) and (32).

Finally, it is advisable that the length of a section may be limited to a few wave lengths because of the attenuation of currents (see Section IV, below).

2) Drive Coils: The dimensions of the drive coils should be chosen so that their radial thickness is the minimum allowed by the mechanical and thermal stress limits in order to have a good coupling with the sleeve. Their axial width should also be optimized in order to reduce the energy transfer between the neighboring drive coils, while keeping the amplitude of the space harmonics within an acceptable range. Due to consideration of the wave attenuation, the resistances of the drive coils and of their connecting leads should be as small as possible. This may be achieved by reducing the number of turns per coil so as to decrease the space needed for the insulation; however, a low number of turns per coil (and hence a low inductance) increases the capacitance and the current to be handled in the power conditioner.

3) Capacitances: As was mentioned before, each section consists of phase windings having the same frequency. A first choice for the value of the phase capacitor

is obtained from the steady-state relationship:

$$f_j = \frac{1}{2\pi\sqrt{KL'_dC_j}} = \frac{v_j}{2\tau} \tag{34}$$

where f_j is the frequency of the LC circuit in the jth section and L'_d is the total self-inductance of the set of drive coils which is connected to the capacitor. Since the equivalent inductance at the terminals of one phase is different from its self-inductance due to the mutual inductance between phases, a coefficient K is used to account for this effect. C_j is the capacitance per phase in the jth section and τ is the pole-pitch of the machine. Hence the capacitance per phase for the jth section is

$$C_j = \frac{1}{KL'_d}\left[\frac{\tau}{\pi v_j}\right]^2. \tag{35}$$

Since the steady state can never be reached, the values of C_j will be adjusted to produce the maximum ETR in (19) (see also Section IV, below).

The volume of the capacitor bank required for a launcher may be approximately estimated as follows: If one assumes that a 1-kg capacitor can store 1 kJ of energy and that the specific weight of the capacitor is 4000 kg/m^3, the energy density of the capacitor bank is about 4 MJ/m^3, a relatively small volume.

4) Voltage Levels: The ETR from (19) determines the amount of energy which must be stored in the capacitor in order to get a specified amount of kinetic energy. The voltage levels are then obtained from the following equations:

$$\frac{1}{2}C_jV_c^2 = \frac{W_{kj}}{\text{ETR}} \tag{36}$$

where W_{kj} is obtained from (30). The initial voltage on each capacitor in the jth section is

$$V_c^j = \sqrt{\frac{2W_{kj}}{C_j \cdot \text{ETR}}}. \tag{37}$$

5) Time Sequences for Switches: As mentioned in the previous section, the traveling wave on the barrel is realized by energizing the drive coils in a certain time sequence. This requires that we predetermine the time sequence for every switch.

According to (34), for an m-phase machine the time interval between two phases is

$$t_i - t_{i-1} = \frac{2\tau}{mv_j}. \tag{38}$$

Hence, the ith phase in the jth section needs to be energized at a time t_i such that

$$t_i = t_{i-1} + \frac{2\tau}{mv_j}. \tag{39}$$

In three-phase machines phase C may be fired at 1/6 of a period (60°) after A with a negative voltage, instead of at 1/3 of a period (120°) later with a positive voltage.

IV. Numerical Results and Discussion

A. Highlights of Results

A capacitively driven four-section coil launcher which is currently being built is used as an example. The dimensions of the launcher are given in Table I and the simulation results are given in Table II. A four-section barrel with a total length of 1.8 m was designed to accelerate a 127-g aluminum projectile from zero initial velocity to a muzzle velocity of 1000 m/s when the total initial energy stored in the capacitor bank is 122 kJ. The total ohmic loss depends on the conductivity of the aluminum. With some degree of pre-cooling, enough to increase the conductivity from $\gamma_{20°C}$ to 1.71 $\gamma_{20°C}$, the total ohmic loss is about 24 percent and the kinetic energy gain in one shot is about 52 percent, yielding a Capacitor Discharge Ratio (CDR) of 76 percent. The remaining 24 percent can be utilized in subsequent shots. (If no pre-cooling is used, the ohmic loss is about 36 percent, with an ETR of 43 percent.) Details of the analysis are discussed in the following paragraphs.

B. Starting Section

The starting section consists of six drive coils spanning one full wavelength (20 cm) and is connected in a three-phase configuration. Each phase is energized with a separate capacitor. A total of 14.5 kJ is initially stored in the three-phase capacitors, with different voltages on each. This was necessary in order to achieve equal-amplitude currents in each of the phase windings. Otherwise the delay in firing phases B and C and the asymmetrical mutual inductances between phases result in unequal current amplitudes. The length of the aluminum sleeve equals the length of this section (or one wavelength); the thickness is 1.5 mm and the weight is 127 g. Initially, the left end of the sleeve is positioned at the left end of the barrel. The dependence of the three-phase currents on time is shown in Fig. 3. Phase A is switched on at $t = 0$, then 60° later phase C with a negative initial voltage, and then phase B follows 60° after phase C. The frequency and phase-shift variations are caused by asymmetries in the mutual inductances between the phases due to the shortness of the section. The waveshapes improve as the length of the section increases, as shown in Fig. 4 for the longer last section (60 cm).

Current buildup in the sleeve can be observed in Fig. 5. Fig. 5(a) shows the current distributions in the sleeve at different instants of time: $t = 0^+$, 0.033, 0.067, and 0.1 ms with only phase A switched on (phases C and B will be switched on at $t = 0.12$ and 0.24 ms, respectively). Comparison with Fig. 5(c) shows that at $t = 0.1$ ms the sleeve current nearly approaches its peak, and this gives a sleeve time constant of a fraction of a millisecond. The initial position of the sleeve is significant. Asymmetries in the induced current distribution along the sleeve disappear, as shown in Fig. 5(b), when the sleeve is initially placed 5 cm to the left of the position as compared with Fig. 5(a) so that both drive coils in phase A are nearly

TABLE I
DIMENSIONS OF AN 1 km/s FOUR-SECTION LAUNCHER*

Section one:		
	Length	20 cm
	Number of coils	6 (15 turns/coil)
	Radial thickness of coil	1.5 cm
	Axial length of coil	3 cm
	Average Radius	3.425 cm
Sections two, three and four have same cross section but different lengths and coils:		
	Length (section 2,3,4)	40 cm, 60 cm, 60cm
	Number of coils (section 2,3,4)	12, 18, 18 (10 turns/coil each)
	Radial thickness of coil	1 cm
	Axial length of coil	3 cm
	Average Radius	3.175 cm
Sleeve:	Length	20 cm
	Average radius	2.5 cm
	Radial thickness	1.5 mm
	Material	aluminum
	Weight	127 g
Clearance between sleeve and barrel coils		1 mm

*The barrel consists of four sections with a total length of 1.8 m. The coils in a section are connected in three phases with a pole pitch τ of 10 cm.

TABLE II
SUMMARY OF SIMULATION RESULTS

parameters	section #1	section #2	section #3	section #4	system results
stored capacitor energy (kJ)	14.5	25	41	41.5	122
peak capacitor voltage (kV)	4.5, 3.7 3.3	12, 9.3 7.6	24.9, 22.8 21.1	32.5, 29.4 27.1	
peak current in drive coils(kA)	25.8	36.3	31.3	31.4	
exit velocity (m/s)	274.2	553.4	831.4	1000	1000
average sleeve (°C) temperature rise	35.04	34.52	30.26	28.92	128.74
energy transfer ratio (%)	32.98	57.93	58.9	47.05	51.58
energy loss ratio (%)	41	28.73	20.49	18.65	23.99
capacitor discharge ratio (%)	73.98	86.66	79.39	65.7	75.57
capacitance (μF)	3X643	3X174.7	3X51.75	3X31.35	3X900.8
frequency (kHz)	1.47	2.75	4.01	5.13	
travel time (ms)	0.96	0.83	0.923	0.703	3.416
section length in units of pole pitch	2 τ	4 τ	6 τ	6 τ	18 τ

equally spaced from the ends of the sleeve. The distribution of the sleeve currents after all three-phase windings have been energized is shown in Fig. 5(c). One can see that a distorted traveling wave is moving from the left to right. The distortion is caused by the space harmonics of the drive coils. Nevertheless, a relatively smooth acceleration is achieved in the first section, as shown in Fig. 6. The projectile accelerates in the first section of the barrel from an initial velocity of zero up to 274.2 m/s. Of the 14.5 kJ initially stored in the capacitors of this section, at exit from the section 33 percent has been transferred into kinetic energy, and 41 percent has been dissipated as ohmic loss. This means that 74 percent of the

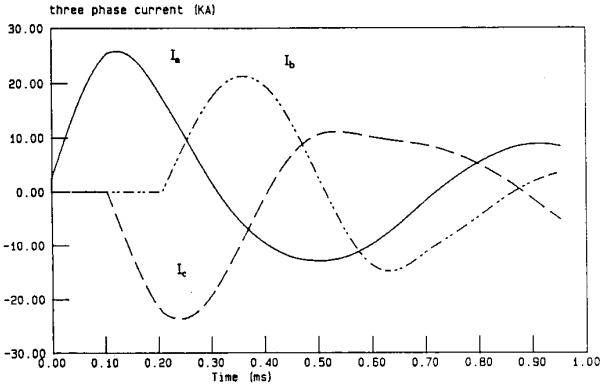

Fig. 3. Currents in the three-phase windings in the starting section.

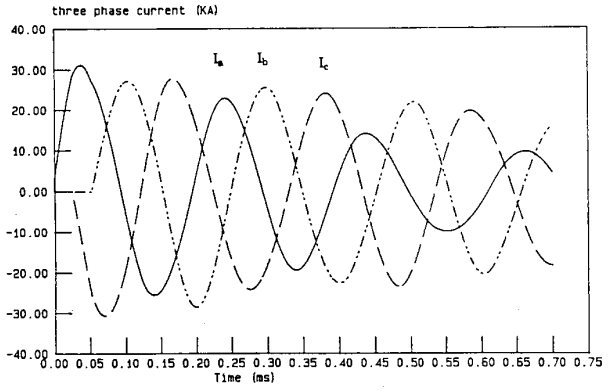

Fig. 4. Currents in the three-phase windings in the last section.

energy initially stored in the capacitors has been discharged. The average temperature rise of the sleeve in the starting section is about 35°C. More information about the first section is given in Table II.

C. Section-to-Section Transition

A smooth transition from one section to the next can be obtained only when the phase shift between the traveling waves generated by the currents in the drive and projectile coils is maintained at a constant level. However, in a capacitively driven coil launcher, a traveling wave cannot be formed until all the three-phase windings of the section are fully energized. For a brief interval of time during the transition the leading section is single phased. This may result in a change of sign in the accelerating force during the transition and may lead to instability. It is possible, however, to alleviate the problem and to achieve a relatively smooth transition from one section to the next by carefully selecting the phase relations in the currents flowing in the drive coils of the two sections. Fig. 7 shows the force and velocity profiles obtained after a few trials for the four-section launcher. The force on the sleeve is relatively smooth within a section, but the transition introduces a slightly negative force.

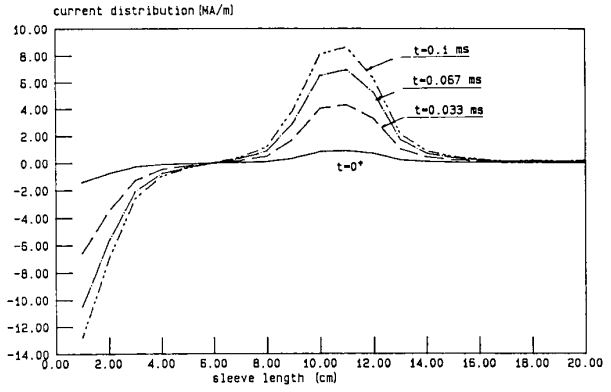

(a)

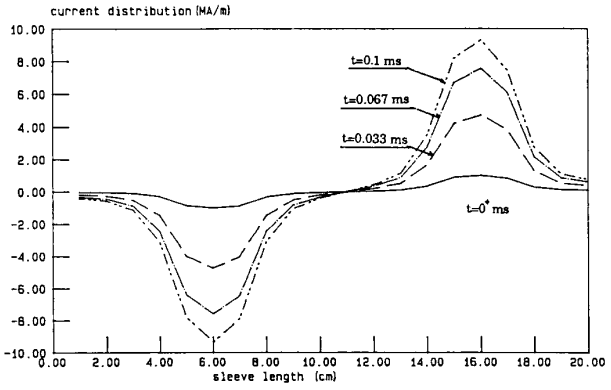

(b)

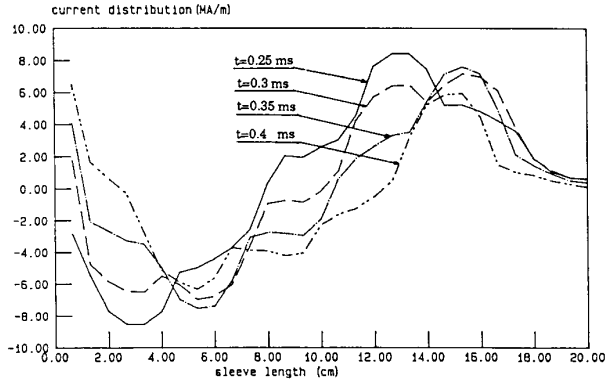

(c)

Fig. 5. (a) Buildup of sleeve current in the starting section. Only phase A is energized. Left end of sleeve coincides with left end of barrel. (b) Buildup of sleeve current in the starting section. Only phase A is energized, but sleeve is initially placed 5 cm to the left. (c) Buildup of sleeve current in the starting section. All three-phase windings have been energized. Sleeve is moved 5 cm to the right.

D. Ohmic Loss and Temperature Rise

Ohmic losses occur both in the drive coils and sleeve. Simulation has shown that the ohmic loss in the drive coils does not cause a serious temperature rise problem because of the short operating time. In the sleeve it is a different matter. Since the current induced in the sleeve is not distributed uniformly and the time constant of thermal diffusion is usually longer than the transit time of the projectile, the cumulative temperature rise in the sleeve is nonuniform. An end-effect may also cause the temperature to peak at the two ends of the sleeve, as shown in Fig. 8. One way to reduce this temperature-peaking effect would be to increase the thickness of the sleeve at the two ends, and in so doing add mechanical strength. The dependence of total ohmic loss in the first section and temperature rise in the sleeve on the thickness of the sleeve is shown in Fig. 9. The ELR is rather insensitive to the sleeve thickness, but the temperature rise in the sleeve is strongly dependent on its thickness. The sleeve thickness should be chosen so that the ETR is maximized while the temperature rise is kept within allowable limits.

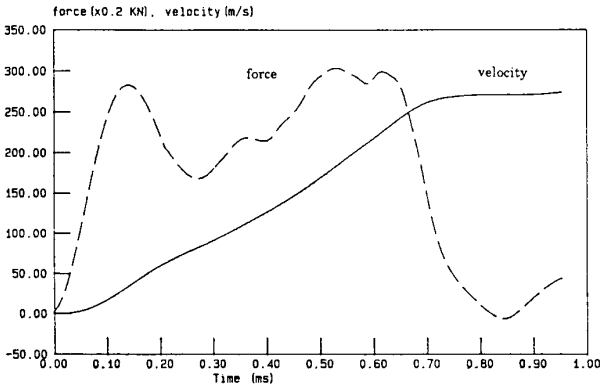

Fig. 6. Force and velocity profiles in the starting section.

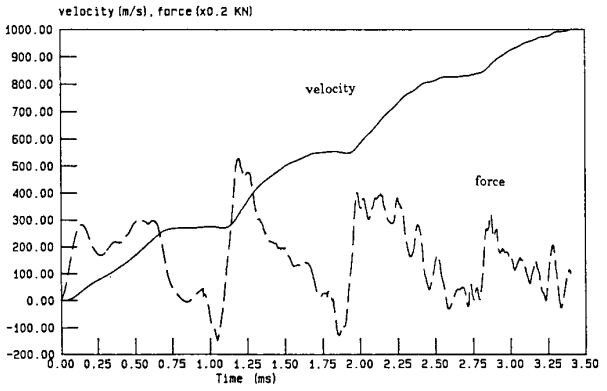

Fig. 7. Force and velocity profiles in the four-section launcher.

E. Skin Effect in the Sleeve

In the previous discussions it was tacitly assumed that the radial current distribution in the sleeve was uniform; that is, that skin depth was not a significant factor. An estimate of the depth of penetration δ may be obtained from

$$\delta \approx \sqrt{\frac{2}{\mu_0 \gamma \omega}} = \sqrt{\frac{2}{\mu_0 \gamma s \omega_s}} = \sqrt{\frac{2\tau}{\pi \mu_0 \gamma s v_s}}. \quad (40a)$$

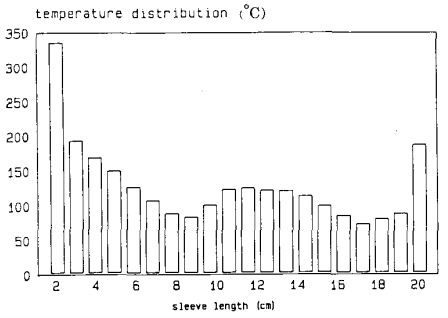

Fig. 8. Distribution of the cumulative average temperature rise in the sleeve.

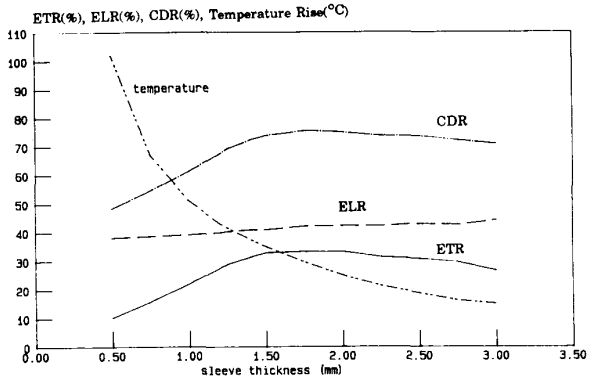

Fig. 9. Energy transfer ratio (ETR), energy loss ratio (ELR), capacitor discharge ratio (CDR), and sleeve temperature rise versus sleeve thickness for starting section. Stored capacitor energy is 14.5 kJ. Frequency is about 1750 Hz.

For $\mu_0 = 4\pi \times 10^{-7}$ H/m, $\gamma = 5 \times 10^7$ mho/m, $\tau = 0.1$ m, δ becomes

$$\delta = \frac{1}{10\pi\sqrt{sv_s}}. \tag{40b}$$

The expression for δ shows that the depth of penetration in the sleeve depends on the slip frequency $s\omega_s$, and hence on the slip velocity sv_s. For the best usage of the sleeve material the current distribution in the radial direction should be relatively uniform, and therefore the simulation model used in this paper should not lead to a significant error. A relatively uniform current distribution is achieved when the sleeve thickness is small as compared with the skin depth δ. It follows that the frequency in each section should be always chosen so that the slip is sufficiently small in order to satisfy the condition stated above. Another reason for selecting a small slip is that the heat loss is proportional to s.

For the 1 km/s example (see below) we used here, the minimum depth of penetration in the 1.5-mm-thick sleeve occurs at the time when the sleeve enters each section as shown in the data in Table III. Thus in each section, even at entry, the minimum skin depth exceeds the sleeve thickness and the effect of radial nonuniformity is probably small.

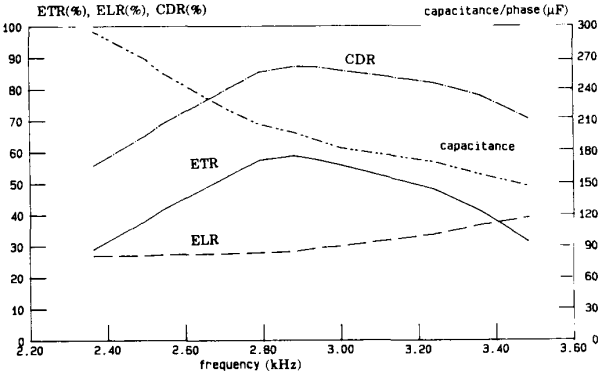

Fig. 10. Energy transfer ratio (ETR), energy loss ratio (ELR), capacitor discharge ratio (CDR), and capacitance versus the resonant frequency for the second section. Stored capacitor energy is 25 kJ.

TABLE III
DEPENDENCE OF SKIN DEPTH ON FREQUENCY FOR SLEEVE OF AN 1 km/s GUN

parameters	section 1	section 2	section 3	section 4
frequency (Hz)	1470	2750	4010	5130
sync. velocity (m/s)	294	550	802	1026
entering slip	1	0.5	0.31	0.19
depth of penetration > (mm)	1.86	1.92	2.02	2.28

F. Energy Transfer From Capacitors to the Projectile

As we mentioned before, the major objective in designing a capacitively driven coil launcher is to convert as much as possible of the energy stored in the capacitors into kinetic energy of the projectile. A low-energy conversion ratio may result from one of the following:

1) Failure to produce a proper traveling magnetic wave on the barrel.
2) Poor coupling between drive coils and the sleeve.
3) Improper resonant frequency impressed on the section.
4) Improper sleeve dimensions and material conductivity.

The dependence of the ETR on the resonant frequency of the second section is shown in Fig. 10, where one can see that the ETR varies from about 25 to 59 percent as the resonant frequency changes from 2.3 to 3.5 kHz. The ETR also strongly depends on the sleeve thickness, as shown in Fig. 9. A thin sleeve gives a large resistance and high temperature rise while a thick sleeve yields a long time constant and slow current buildup. Both extremes result in a poor energy transfer ratio, as shown in Fig. 9.

V. COMPARISON BETWEEN THEORETICAL PREDICTIONS AND EXPERIMENTAL RESULTS

A small one-section demonstration model of a capacitively driven coil launcher was built. Its parameters are given in Table IV. Measured and calculated voltage and current waves are shown in Figs. 11 and 12. Agreement between the two is seen to be very good. Agreement between the measured and calculated muzzle velocities, given in Table IV, is also very good.

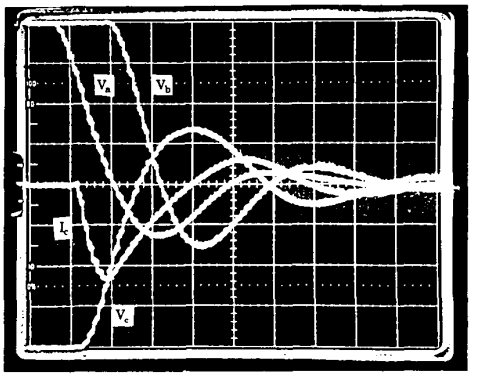

Fig. 11. Oscillogram of three-phase voltages and one-phase current for small laboratory model. Refer to Fig. 12. (Scales: 100 V, 50 A, 1 ms/div.)

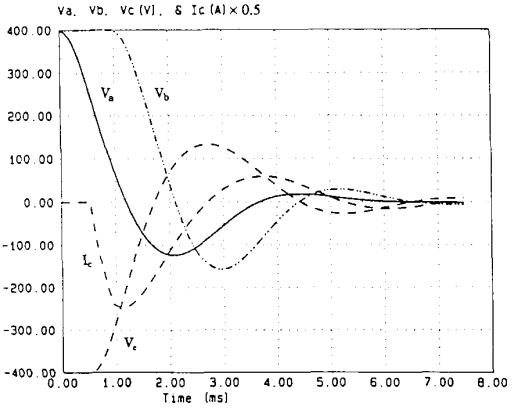

Fig. 12. Computer simulation of three-phase voltages and one-phase current for small laboratory model. Refer to Fig. 11.

TABLE IV
SMALL LABORATORY MODEL (REFER TO FIGS. 11 AND 12)

Barrel consists of one section with a total length of 20 cm, and the coils are connected in three phase with a pole pitch of 6.75 cm:	
Number of coils	6 (100 turn/coil)
Radial thickness of coil	0.75 cm
Axial length of coil	2.25 cm
Coil inner diameter	6.7 cm
Sleeve dimensions:	
Length	13.5 cm
Radial thickness	0.17 cm
Outer diameter	6.2 cm
Material	aluminum
Weight	118 g
Capacitors used as power supply:	
Capacitance	288 μF/phase
Initial Capacitor voltage	400 V/phase
Muzzle velocity (calculated)	3.5 m/s
Muzzle velocity (measured)	3.46 m/s

VI. COMPARISON BETWEEN TRANSIENT AND STEADY-STATE DESIGN APPROACHES

It is of interest to compare two designs for the same launcher: One based on the transient approach, as presented in this paper, and the other on a steady-state approach, presented earlier [4]. Table V provides a few results for comparison.

TABLE V
DATA COMPARISON FOR AN 1 km/s FOUR-SECTION LAUNCHER DERIVED FROM TWO DIFFERENT DESIGN SCHEMES

Results / Design Basis	Total Transit Time	Average Sleeve Temp.	Cap/Ph in 3rd Sec.	Init. Peak Volt/Ph 3rd Sec.	Peak Curr per Ph. 3rd Sec.
Transient (see Table 2)	3.42 ms	128.7°C	51.8 μF	22.8 kV	31.3 kA
Steady-State (see ref. [4])	3.71 ms	143.6°C	82.8 μF	20.4 kV	40.6 kA

It should also be noted that the steady-state design procedure requires that several preliminary assumptions be made, such as ETR, average acceleration, and equivalent phase inductance. These must be based on experience and insight into the launcher operation [4]. Although the steady-state design procedure is much simpler, the transient approach provides a more detailed and accurate result.

VII. CONCLUDING REMARKS

A lumped-parameter computer model of the coil launcher gave performance predictions which agree with the experimental data obtained with a small-scale prototype that was built in the laboratory for proof-of-principle. The model is a useful design tool, specifically with regard to the dimensioning of the coils and sleeve, and the sizing of section lengths and phase capacitors. It also helps in establishing the proper phasing-in of successive sections so that the transition is relatively smooth. Although a complete design has been performed only for the 1 km/s gun now under construction, preliminary calculations suggest that muzzle velocities in the range of 6 km/s could be achieved with a relatively minor development effort. However, at higher velocities it is expected that a major effort to develop new types of switching elements will be required.

ACKNOWLEDGMENT

The authors would like to thank Prof. Y. Naot, H. K. Jung, H. P. Lee, P. Joshi, X. N. Lu, Q. C. Gu, and G. H. Fan for their contributions to the experimental work and for their valuable discussions.

REFERENCES

[1] M. D. Driga, W. F. Weldon, and H. H. Woodson, "Electromagnetic induction launchers," *IEEE Trans. Magn.*, vol. MAG-22, pp. 1453-1458, Nov. 1986.

[2] P. Mongeau, W. Snow, G. Colello, P. Rezza, and H. Kolm, "Coilgun technology evolution," presented at the 4th Symp. on Electromagnetic Launcher Tech., Austin, TX, Apr. 12-14, 1988.

[3] D. G. Elliot, "Traveling-wave inductive launchers," presented at the 4th Symp. on Electromagnetic Launcher Tech., Austin, TX, Apr. 12-14, 1988.
——, *IEEE Trans. Magn.*, vol. 25, pp. 159-163, Jan. 1989.

[4] Z. Zabar, Y. Naot, L. Birenbaum, E. Levi, and P. N. Joshi, "Design and power conditioning for the coil-gun," presented at the 4th Symp. on Electromagnetic Launcher Tech., Austin, TX, Apr. 12-14, 1988.
——, ——, ——, ——, and ——, *IEEE Trans. Magn.*, vol. 25, pp. 627-631, Jan. 1989.

[5] T. J. Burgess, E. C. Cnare, W. L. Oberkampf, S. G. Beard, and M. Cowan, "The electromagnetic θ gun and tubular projectiles," *IEEE Trans. Magn.*, vol. MAG-18, pp. 46-59, Jan. 1982.

[6] F. W. Grover, *Inductance Calculations.* New York: Dover, 1973.

[7] T. H. Fawzi and P. E. Burke, "The accurate computation of self and mutual inductance of circular coils," *IEEE Trans. Power App. Syst.*, vol. PAS-97, pp. 464-468, Mar./Apr. 1978.

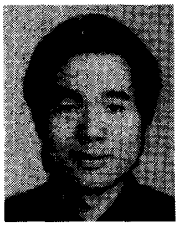

Jianliang He (S'89) was born in Jiangsu, China, on December 27, 1954. He graduated from the Department of Electrical Engineering, Xian Jiaotung University, Xian, China, in 1977. He worked at the same University from 1977 to 1981. He received the M.S. degree from Rensselaer Polytechnic University, Troy, NY, in 1985. Since January 1985 he has been working towards obtaining the Ph.D. degree in energy conversion at the Polytechnic University, Brooklyn, NY, where currently he is a Research Associate.

*

Enrico Levi (M'58-SM'58-LS'89) is a graduate of the Technion-Israel Institute of Technology, and received the Ph.D. degree in electrical engineering from the Polytechnic University, Brooklyn, NY.

He is Professor Emeritus of Electrophysics at the Polytechnic University, and is President and Treasurer of Enrico Levi, Inc. He has been a Visiting Professor and has lectured in many universities in the United States and abroad, and has served as a Consultant to the U.S. Department of Energy, NASA, the Argonne National Laboratory, the Lawrence Livermore Laboratory, and many industrial firms.

Dr. Levi's published work includes: *Electromechanical Power Conversion* (1982); *Polyphase Motors: A Direct Approach to Their Design* (1984); chapters in *Magnetohydrodynamic Electric Power Generation* (1978); *Standard Handbook for Electrical Engineers* (1986); *The Encyclopedia of Physical Science and Technology* (1986); and more than 50 papers in technical and scientific journals. He also holds two patents. He is a recipient of the Sigma Xi Distinguished Faculty Research Citation, the IEEE Charles J. Hirsch Award, and the Lady Davis Fellowship, and is a member of Tau Beta Pi and Sigma Xi.

*

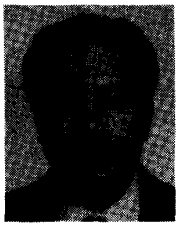

Zivan Zabar (M'76-SM'81) was born in Hadera, Israel, in 1939. He received the B.Sc., M.Sc., and Sc.D. degrees from the Technion-Israel Institute of Technology in 1965, 1968, and 1972, respectively.

He is currently Professor of Electrical Engineering at the Polytechnic University in Brooklyn, NY. His areas of interest are power electronics and electrical power systems.

Dr. Zabar holds two patents and has published many papers in technical journals. He is a member of Sigma Xi.

*

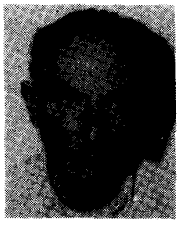

Leo Birenbaum (S'45-A'48-M'55-SM'70) was born in New York City in 1927. He received the B.E.E. degree from the Cooper Union, New York, in 1946, the M.E.E. degree from the Polytechnic Institute, Brooklyn, NY, in 1958, where he obtained the M.S. degree in physics in 1974.

He is now Research Associate Professor at the Polytechnic, where, since 1951, he has done research and taught electrical engineering. He has worked and published in the areas of microwaves, biological effects of magnetic fields, linear motors, and power distribution.

Mr. Birenbaum is a member of the New York Academy of Sciences and the Bioelectromagnetics Society.